SCATTERING ANALYSIS AND SYNTHESIS
OF WAVE TRAINS

R. J. SOBEY[1] and E. J. COLMAN[2]

Abstract

The Zakharov-Shabat scattering transform is an exact solution technique for the nonlinear Schrödinger equation, which describes the time evolution of weakly nonlinear wave trains. Envelope soliton and uniform wave train solutions of the nonlinear Schrödinger equation are separable in scattering transform space. The scattering transform is a potential analysis and synthesis technique for natural wave trains. Discrete versions of the direct and inverse scattering transform are presented, together with proven algorithms for their numerical computation from typical ocean wave records. The consequences of discrete resolution are considered.

1. Introduction

The potential of the nonlinear Schrödinger equation and the Zakharov-Shabat scattering transform as an analysis technique for natural wave trains has been argued by Sobey and Colman [15]. The nonlinear Schrödinger equation describes the evolution of weakly nonlinear wave trains in deep water, retaining a measure of nonlinearity and leading to both envelope soliton and uniform wave train solutions. Steep wave forms interact in a nonlinear manner, complicating the separation of the fundamental components or normal modes and invalidating linear superposition and the Fourier transform or variance spectrum representation of a natural sea state. Under certain circumstances, however, the nonlinear normal modes are separable in scattering transform space, just as the linear normal modes are separable in Fourier transform space. The scattering data in

[1] Department of Civil and Systems Engineering, James Cook University, Townsville, Queensland 4811.
[2] Woodside Offshore Petroleum Pty. Ltd , Perth, Western Australia 6000.

scattering transform space is time invariant and analogous to the Fourier spectrum for the linear problem. The inverse scattering transform is also defined, allowing synthesis of consistent sea states in a manner analogous to the inverse Fourier transform. In addition, the inverse scattering transform accommodates consistent time evolution of the initial wave train.

Following a brief review of the background to the nonlinear Schrödinger equation and the Zakharov-Shabat scattering transform, an implementation is described of the discrete direct scattering transform and the discrete inverse scattering transform in the context of typical ocean wave records.

2. The nonlinear Schrödinger equation

The classical approach to representation of the nonlinearity of surface gravity waves in deep water has been the Stokes expansion, in which the smallness of the wave steepness is exploited to linearise the equations and estimate nonlinear influences as small corrections to the linear wave solution. This approach has proved reasonably successful but the linearisation removes potentially fundamental aspects of the problem.

A number of more recent studies of the evolution of nonlinear wave trains in deep water and in one spatial dimension have retained weak nonlinearity in the lowest order equations by requiring a balance between two small parameters, the wave steepness ka and the spectral narrow-bandedness $\Delta k/k$, where k is the wave number and a the wave amplitude. It is convenient to extract the central, dominant or carrier wave (frequency ω_0, wave number k_0, where $\omega_0^2 = gk_0$) and focus attention on the slowly varying complex wave envelope $A(x, t)$ which is related to the free water surface $H(x, t)$ as

$$H(x, t) = \mathrm{Re}\big[A(x, t)\exp\{i(k_0 x - \omega_0 t)\}\big], \tag{2.1}$$

where x represents position and t time. The resulting lowest order equation is the nonlinear Schrödinger equation

$$i\left(\frac{\partial A}{\partial t} + \frac{\omega_0}{2k_0} \frac{\partial A}{\partial x} \right) - \frac{\omega_0}{8k_0^2} \frac{\partial^2 A}{\partial x^2} - \tfrac{1}{2}\omega_0 k_0^2 |A|^2 A = 0, \tag{2.2}$$

describing evolution in space and time of the envelope of a weakly nonlinear wave train in deep water. A simple cubic nonlinearity appears in the final term. Equation (2.2) was first established by Zakharov [18] and subsequently confirmed by Hasimoto and Ono [9], Davey and Stewartson [6] and Yuen and Lake [17].

Introducing dimensionless variables $\tau = -\omega_0 t$, $s = 2\sqrt{2}\, k_0(x - \omega_0 t/2k_0)$ and $u(s, \tau) = k_0 A(x, t)/4$ gives

$$i\frac{\partial u}{\partial \tau} + \frac{\partial^2 u}{\partial s^2} + 8\,|\,u\,|^2 u = 0, \tag{2.3}$$

as the standard dimensionless form of the nonlinear Schrödinger equation; $u(s, \tau)$ being the dimensionless complex envelope in a co-ordinate system now moving with the group velocity $\omega_0/2k_0$ of the dominant wave.

As for linear wave theory, there are uniform wave train or sine wave solutions to the nonlinear Schrödinger equation. In dimensional terms,

$$H(x, t) = a_0 \sin\left[k_0 x - \omega_0\left(1 + \tfrac{1}{2}k_0^2 a_0^2\right)t\right], \tag{2.4}$$

or in dimensionless terms

$$u(s, \tau) = \varepsilon \exp(i8\varepsilon^2 \tau). \tag{2.5}$$

The amplitude ε of the dimensionless wave envelope is related to the wave steepness as $\varepsilon = k_0 a_0/4$. The wave envelope modulates at a frequency of $8\varepsilon^2$, which is also related to the wave steepness.

There are also envelope soliton solutions to the nonlinear Schrödinger equation:

$$u(s, \tau) = 2\eta \exp\left[-i\{4(\xi^2 - \eta^2)\tau + 2\xi s - \theta\}\right]\mathrm{sech}\left[2\eta(s - s_0 + 4\xi\tau)\right]. \tag{2.6}$$

This complex envelope has a dimensionless amplitude of η, a dimensionless half width of $\ln(2 - \sqrt{3})2\eta$ and moves at a dimensionless speed of 4ξ relative to the group velocity of the dominant wave of the train. The hyperbolic secant profile oscillates at a dimensionless angular frequency of $4(\xi^2 - \eta^2)$ and a dimensionless wave number of 2ξ. It is defined by four independent dimensionless parameters; η, ξ, s_0 and θ. In dimensionless terms the water surface profile is given by

$$H(x, t) = a\,\mathrm{sech}\left[\sqrt{2}\, k_0^2 a\{(x - x_0) - (\omega_0/2k_0 + v)t\}\right]$$

$$\times \exp\left[-\frac{i}{4}k_0^2 a^2 \omega_0 t - \left(4ik_0^2/\omega_0\right)v\{(x - x_0) - (\omega_0/2k_0 + v)t + \theta\}\right], \tag{2.7}$$

where a characterises the amplitude and v the velocity relative to the group velocity of the dominant or carrier wave; x_0 and θ represent position and phase. Equation (2.7) describes a wave packet oscillating at the dominant wave frequency and wave number but amplitude modulated by the hyperbolic secant profile. Envelope solitons are uniquely nonlinear wave forms, the stability of the wave packet being achieved by a balance between nonlinear and dispersive influences.

3. The scattering transform

The scattering transform is applicable to a certain class of nonlinear partial differential equations of evolution. It was first applied to the Korteweg-de Vries equation by Gardner *et al.* [8] and extended to the nonlinear Schrödinger equation by Zakharov and Shabat [19]. The close analogy with the solution of a linear partial differential equation of evolution by the Fourier transform (or indeed any integral transform) has been drawn by Ablowitz *et al.* [1].

The solution of the nonlinear Schrödinger equation can be represented (see Figure 1) as

$$u(s,0) \underset{\text{I}}{\to} S(\zeta,0) \underset{\text{II}}{\to} S(\zeta,\tau) \underset{\text{III}}{\to} u(s,\tau). \tag{3.1}$$

The initial data is mapped into scattering transform space in step I by the direct scattering transform, appropriate time evolution is accomplished in scattering transform space by step II and the mapping is reversed to physical space in step III by the inverse scattering transform. The representation $S(\zeta, \tau)$ in scattering transform space is called the scattering data, which is analogous to the Fourier transform in Fourier transform space. It is fundamental to the Zakharov-Shabat scattering transformation that each of the three steps in Equation (3.1) is a separate linear problem, the solution of the nonlinear Schrödinger equation being decomposed into a sequence of linear problems. It is also fundamental that the free wave (continuous spectrum) and soliton components (discrete spectrum) are separable from the scattering data and that these normal modes are time invariant.
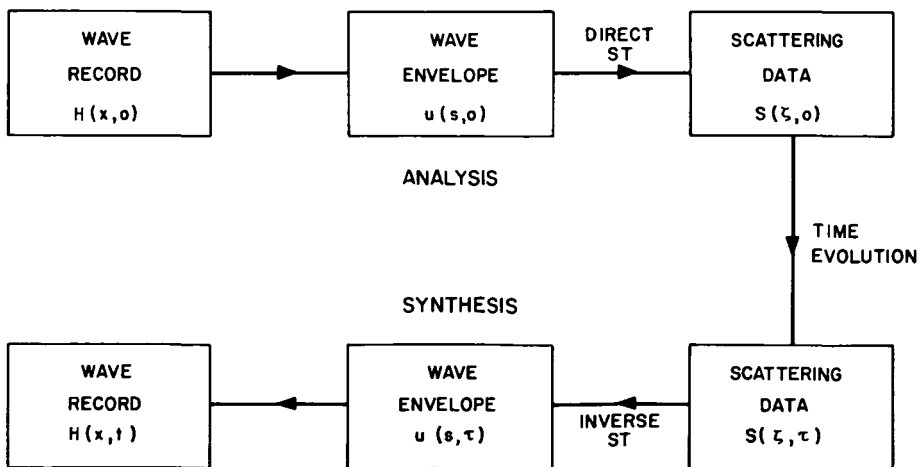

Figure 1. Analysis and synthesis of weakly nonlinear waves.

4. Direct scattering problem

The direct scattering problem involves the solution of the Zakharov-Shabat eigenvalue problem which can be reduced, [19], to the simultaneous linear partial differential equations

$$\frac{\partial v_1}{\partial s} + i\zeta v_1 = q v_2,$$
$$\tag{4.1a}$$

$$\frac{\partial v_2}{\partial s} - i\zeta v_2 = -q^* v_1,$$
$$\tag{4.1b}$$

where the eigenfunctions are the vectors

$$v = \begin{bmatrix} v_1(s; \tau, \zeta) \\ v_2(s; \tau, \zeta) \end{bmatrix}$$

which have complex eigenvalues $\zeta = \xi + i\eta$. In application, time τ and the eigenvalues ζ are constant parameters of the problem, so that equations (4.1) become ordinary differential equations. The scattering potential $q(s; \tau) = 2iu(s; \tau)$ is the representation of the complex dimensionless wave envelope $u(s; \tau)$ and the asterisk superscript indicates the complex conjugate. The time invariant asymptotic characteristics of the eigenfunctions form a sufficient basis for the reconstruction of the scattering potential and subsequently the wave record at any future time. These asymptotic characteristics comprise the scattering data, form-ing a complete summary of the wave data in scattering transform space, analo-gous to the linear Fourier spectrum. For real eigenvalues $\zeta = \xi$, Zakharov and Shabat define two pairs of linearly independent eigenfunction solutions of Equation (4.1), ϕ, $\bar{\phi}$ and ψ, $\bar{\psi}$, termed the Jost functions, which have the asymptotic characteristics

$$s = -\infty \qquad\qquad\qquad\qquad\qquad\qquad s = \infty$$

$$\begin{bmatrix} e^{-i\zeta s} \\ 0 \end{bmatrix} \quad \leftarrow \quad \phi(s; \tau, \zeta) = \begin{bmatrix} \phi_1 \\ \phi_2 \end{bmatrix} \quad \rightarrow \quad \begin{bmatrix} ae^{-i\zeta s} \\ be^{i\zeta s} \end{bmatrix}, \tag{4.2a}$$

$$\begin{bmatrix} 0 \\ -e^{i\zeta s} \end{bmatrix} \quad \leftarrow \quad \bar{\phi}(s; \tau, \zeta) = \begin{bmatrix} \phi_2^* \\ -\phi_1^* \end{bmatrix} \quad \rightarrow \quad \begin{bmatrix} b^* e^{-i\zeta s} \\ -a^* e^{i\zeta s} \end{bmatrix}, \tag{4.2b}$$

$$\begin{bmatrix} b^* e^{-i\zeta s} \\ ae^{i\zeta s} \end{bmatrix} \quad \leftarrow \quad \psi(s; \tau, \zeta) = \begin{bmatrix} \psi_1 \\ \psi_2 \end{bmatrix} \quad \rightarrow \quad \begin{bmatrix} 0 \\ e^{i\zeta s} \end{bmatrix}, \tag{4.2c}$$

$$\begin{bmatrix} a^* e^{-i\zeta s} \\ -be^{i\zeta s} \end{bmatrix} \quad \leftarrow \quad \bar{\psi}(s; \tau, \zeta) = \begin{bmatrix} \psi_2^* \\ -\psi_1^* \end{bmatrix} \quad \rightarrow \quad \begin{bmatrix} e^{-i\zeta s} \\ 0 \end{bmatrix}. \tag{4.2d}$$

The scattering data are the coefficients $a(\zeta)$ and $b(\zeta, \tau)$ relating these two sets of linearly independent solutions at the opposite asymptotic state, as

$$\bar{\phi} = a\psi + b\bar{\psi}, \tag{4.3a}$$

$$\bar{\phi} = a^*\psi + b^*\bar{\psi}, \tag{4.3b}$$

$$\bar{\psi} = -a\bar{\phi} + b^*\bar{\phi}, \tag{4.3c}$$

and

$$\bar{\psi} = a^*\phi + b\bar{\phi}, \tag{4.3d}$$

from which it follows that

$$aa^* + bb^* = 1. \tag{4.4}$$

The existence of the scattering transform is subject to the condition

$$\int_{-\infty}^{\infty} |q|\, ds < \infty, \tag{4.5}$$

which requires that the scattering potential decay sufficiently rapidly as $|s| \to \infty$. When this condition is satisfied, the eigenfunctions and the scattering data can be extended into the upper half of the complex ζ plane, $\eta \geq 0$. The eigenvalues are continuous along the real axis $\zeta = \xi$, and there are a discrete number, say N, corresponding to zeroes of the $a(\zeta)$ function in the upper half plane. Each of these discrete complex eigenvalues ζ_j, $j = 1, 2, \ldots, N$, corresponds to a soliton whose complete scattering data representation is $b(\zeta_j, \tau)$. Correspondingly, the continuous eigenvalues ξ along the real axis are identified, [1], with the free wave or radiation components and their complete scattering data is given by both $a(\xi)$ and $b(\zeta, \tau)$. For the continuous and discrete eigenvalues, the scattering data $S(\zeta, \tau)$ is defined as

$$S(\zeta, \tau) = S\left[\frac{b(\xi, \tau)}{a(\xi)}; \zeta_j, c_j(\zeta_j, \tau) = \frac{b(\zeta_j, \tau)}{a'(\zeta_j)}, j = 1, 2, \ldots, N\right], \tag{4.6}$$

where $1/a'(\zeta_j)$ is the complex residue of the $1/a(\zeta)$ function at the pole ζ_j. A schematic illustration of the discrete and continuous components of the scattering data spectrum is shown in Figure 2. The discrete spectrum is shown as delta functions, being poles of the $b(\zeta, \tau)/a(\zeta)$ function, but the spectral constants $c_j(\zeta_j, \tau)$ are decidedly finite, being the result of nonzero residues $1/a'(\zeta_j)$.

The nature of the direct scattering problem for the particular solution ϕ, for example, can be discerned from equations (4.1) and (4.2a). Equations (4.1) are an initial value problem describing subsequent development in non-dimensional

space of the eigenfunctions, given an initial state. For the particular solution ϕ, the initial state is the plane wave $\exp(-i\zeta s)$ at $s = -\infty$ which is scattered by the scattering potential $q(s; \tau)$, the wave envelope, as it propagates or radiates in s space, to result in a transmission coefficient $a(\zeta)$ and a reflection coefficient $b(\zeta, \tau)$ at $s = +\infty$. Where the wave envelope or the scattering potential is zero, the plane wave propagates unchanged through space such that the transmission coefficient $a(\zeta)$ is identically one and the reflection coefficient $b(\zeta, \tau)$ is zero. Hence from equation (4.4) it follows that $a(\xi) \to 1$ and $b(\xi, \tau) \to 0$ as $|\xi| \to \infty$. For ζ real, the eigenvalues have the nature of dimensionless wave numbers or phase speeds but they refer to relative motion with respect to the dominant wave with wave number k_0. These eigenvalues are continuous in the range $-\infty < \xi < \infty$, although in practice it would be expected that most of the energy would be concentrated about the dominant wave, $\xi = 0$. A narrow-banded spectrum is also fundamental to the derivation of the nonlinear Schrödinger equation. The discrete eigenvalues are $\zeta_j = \xi_j + i\eta_j$, ξ_j characterising the phase speed of the jth soliton with respect to the dominant wave celerity and η_j characterising its dimensionless amplitude and length.
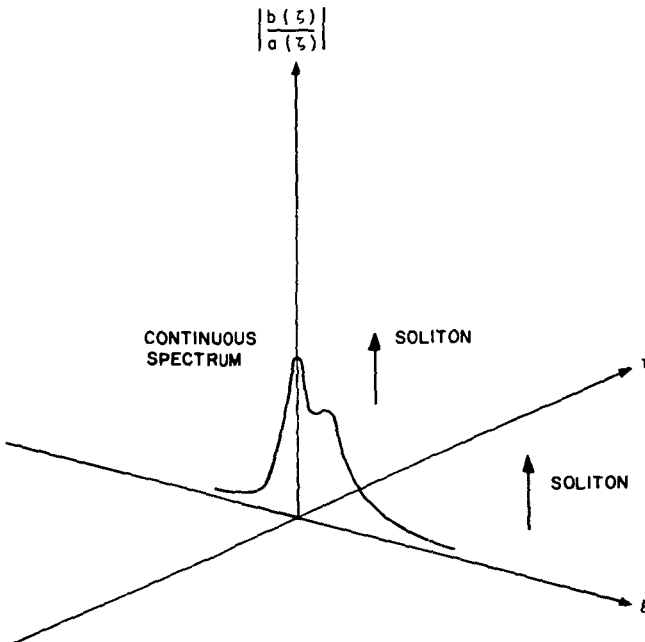

Figure 2. Schematic representation of scattering data spectrum.

5. The discrete scattering transform

Computation of the discrete scattering transform from a real wave record $H(0, t)$ involves the computation of the scattering potential $q(s; 0)$ from the wave record, followed by numerical solution of the Zakharov-Shabat eigenvalue problem to obtain the scattering coefficients $a(\zeta)$ and $b(\zeta, 0)$ and the scattering data spectrum. An initial step is the identification of the dominant wave parameters ω_0 and k_0.

For the present purpose, ω_0 has been equated with the peak frequency of the Fourier spectrum and k_0 is computed subsequently from the dispersion relationship, although it is possible to refine this initial estimate of ω_0 by means of any remaining linear trend in the phase of the estimated complex envelope, as described by Bolt and Brillinger [2].

The complex wave envelope $A(x, 0)$ may be computed from $H(x, 0)$, related to the wave record $H(0, t)$ in a discrete sense as

$$H(m\Delta x, 0) = H(0, m\Delta t), \tag{5.1}$$

where $\Delta x = -\omega_0 \Delta t / 2k_0$ and $m = -M, \ldots, -1, 0, 1, \ldots, M$. The initial data required is the spatial description of the water surface at time zero, but it is the time history of the water surface at position zero that is available from wave records. Equation (5.1) essentially invokes Taylor's hypothesis, [16], utilised in turbulence to relate $H(0, t)$ to $H(x, 0)$. In this context it is a frozen envelope assumption, the hypothesis being that the wave envelope at time zero is convected past the zero position at the group speed of the dominant wave and without change of form. This assumption is in fact exact to lowest order, where only the first and second terms of equation (2.2) remain and the envelope is propagated at the group speed. The time and space origins can be assumed as central to the appropriate records without loss of generality. For a typical wave record, Δt is $0.5s$ and M is 1024.

Adopting a Fourier representation for $H(x, 0)$, it follows directly, [7], that

$$A(x, 0) = \left[H(x, 0) + i\hat{H}(x, 0)\right] \exp(-ik_0 x), \tag{5.2}$$

where

$$\hat{H}(x, 0) = \frac{1}{2\pi} \int_{-\infty}^{\infty} iF(k) \exp(ikx) \, dk, \tag{5.3}$$

and

$$F(k) = \int_{-\infty}^{\infty} H(x, 0) \exp(-ikx) \, dx. \tag{5.4}$$

In complex demodulation of time series, the real function $\hat{H}$ is the Hilbert transform, [7], of H and the term in square brackets is the pre-envelope function. Equations (5.3) and (5.4) are the inverse and direct Fourier transforms in the

space domain and were implemented in their finite discrete forms, using an FFT algorithm. The wave envelope was computed as

$$A(m\Delta x, 0) = [H(m\Delta x, 0) + i\hat{H}(m\Delta x, 0)]\exp(-ik_0 m\Delta x), \qquad (5.5)$$

which was scaled to the finite discrete scattering potential

$$q(m\Delta s) = (2ik_0/4)A(m\Delta x, 0), \qquad (5.6)$$

where

$$\Delta s = 2\sqrt{2}\, k_0 \Delta x.$$

The existence condition for the scattering transform imposed by equation (4.5) is very similar to the existence condition for the Fourier transform, [3],

$$\int_{-\infty}^{\infty} |H(t)|\, dt < \infty. \qquad (5.7)$$

These conditions potentially restrict the respective transforms to wave records that decay sufficiently rapidly as $|t| \to \infty$. Of course, this condition is not satisfied in the nondecaying finite records used in analysis but is accommodated for the Fourier transform by invoking the theory of generalised functions, [11], and using the Dirac comb, [13], and a wide range of possible data windows. An approach akin to the theory of generalised functions may be applicable also to the scattering transform and further clarification of this point is necessary. The approach has nonetheless been adopted, using a cosine taper window to J points at either end of the discrete record of $2M + 1$ points. In discrete Fourier analysis the fraction J/M is normally $1/5$.

The computation of the scattering coefficients requires the numerical solution of the Zakharov-Shabat eigenvalue problem, equations (4.1), to obtain any one of the possible solutions ϕ, $\bar{\phi}$, ψ or $\bar{\psi}$. Simultaneous solution of equations (4.1) with initial conditions given by equations (4.2) yields the scattering coefficients at the other extremity. The particular solution ϕ was chosen for its mathematical convenience and a simple change of variable introduced to simplify the problem:

$$\Phi_1 = \phi_1 \exp(i\zeta S/2), \qquad (5.8a)$$

and

$$\Phi_2 = \phi_2 \exp(-i\zeta S/2), \qquad (5.8b)$$

where S is the length of the finite integration domain, extending from $-S/2$ to $S/2$. Equations (4.1) thus become

$$\frac{d\Phi_1}{ds} = -i\zeta\Phi_1 + q\Phi_2 \exp(i\zeta S), \qquad (5.9a)$$

$$\frac{d\Phi_2}{ds} = i\zeta\Phi_2 - q^*\Phi_1 \exp(i\zeta S), \qquad (5.9b)$$

and the asymptotes become

$$s = -S/2 \qquad\qquad\qquad s = S/2$$

$$\begin{bmatrix} 1 \\ 0 \end{bmatrix} \exp(i\zeta S) \quad \leftarrow \quad \begin{bmatrix} \Phi_1 \\ \Phi_2 \end{bmatrix} \quad \rightarrow \quad \begin{bmatrix} a \\ b \end{bmatrix}, \qquad (5.10)$$

giving initial conditions at $s = -S/2$ of

$$\Phi_1(-S/2) = \exp(i\zeta S), \qquad (5.11a)$$

and

$$\Phi_2(-S/2) = 0. \qquad (5.11b)$$

For numerical integration, the complex solutions Φ_1 and Φ_2 were separated into real and imaginary parts, $\Phi_1 = y_1 + iy_2$ and $\Phi_2 = y_3 + iy_4$, reducing equations (5.9) to a set of four simultaneous first-order ordinary differential equations which were numerically integrated for each value of ζ using the standard fourth-order Runge-Kutta algorithm. As the algorithm requires computation of the derivatives incorporating $q(s)$ at $\frac{1}{2}h$ intervals, a solution step of $h = 2\Delta s$ was adopted so that the discrete scattering potential was available at the locations where the derivative was required. The scattering coefficients $a(\zeta)$ and $b(\zeta, 0)$ were extracted from the final values of the solutions at $s = S/2$, i.e. $a(\zeta) = y_{1_M} + iy_{2_M}$ and $b(\zeta, 0) = y_{3_M} + iy_{2_M}$.

The choice of the ξ and η values is not dictated by the locations of the scattering potentials, but the choice is not entirely free. To lowest order, $\xi = 0$ and the complete wave train is identified with the dominant wave. The range of possible ξ values is thus centred about $\xi = 0$; for convenience a uniform $\Delta\xi$ step (typically 0.005) was chosen with $\xi = r\Delta\xi$ for $r = -R, \ldots, -1, 0, 1, \ldots, R$. The bandwidth $R\Delta\xi$ should be relatively narrow, a large value giving better resolution but at a computational cost. The choice is also related to the discrete resolution parameter $\xi\Delta s$ as subsequently discussed. For exploratory computations $R = M/2$ has been used. The η values were chosen in a similar manner but only the upper half plane is necessary.

With the scattering data computed for a selected range of ζ values in the upper half plane, the zeroes of the $a(\zeta)$ function were located by the specification of a threshold level for the $|1/a(\zeta)|$ surface, exceedance of which identified a pole or discrete eigenvalue $\zeta_j, j = 1, \ldots, N$. With experience in setting the threshold level, systematic scanning of the surface was very effective.

Computation of the continuous spectrum $b(\xi, 0)/a(\xi)$ required simple division of the complex scattering coefficients. The discrete spectrum $b(\zeta_j)/a'(\zeta_j)$ required

in addition the determination of the residue of each of the poles of the $1/a(\zeta)$ function, computed by complex integration, [4], as

$$\frac{1}{a'(\zeta_j)} = \frac{1}{2\pi i} \int_C \frac{1}{a(\zeta)} d\zeta, \tag{5.12}$$

along any closed contour C enclosing only that pole in a positive sense; the trapezoidal rule was used along a rectangular contour symmetrically placed around the pole $\zeta_j = \xi_j + i\eta_j$ and not including other poles.

6. Inverse scattering problem

The inverse scattering problem is the reconstruction of the scattering potential (and hence the wave envelope and wave train) at any time from the scattering data spectrum, $S(\zeta, 0)$. The time evolution of the propagating wave train is represented as time evolution of the scattering data spectrum in scattering transform space. Zakharov and Shabat [19] have shown that, for the continuous spectrum, $a(\xi)$ is time invariant and

$$b(\xi, \tau) = b(\xi, 0)\exp(i4\xi^2\tau), \tag{6.1}$$

and, for the discrete spectrum, $a(\zeta_j)$ is of course zero and

$$b(\zeta_j, \tau) = b(\zeta_j, 0)\exp(i4\zeta_j^2\tau)$$
$$= b(\zeta_j, 0)\exp(8\eta\xi\tau)\exp\left[i4(\zeta^2 - \eta^2)\tau\right]. \tag{6.2}$$

The evolution of $b(\xi, \tau)$ involves a rotation at dimensionless angular speed $4\xi^2$ with the magnitude remaining constant and the evolution of $b(\zeta_j, \tau)$ involves a time-dependent amplitude scaling in addition to a rotation at speed $4(\xi^2 - \eta^2)$. The time evolved scattering data spectrum is

$$S(\zeta, \tau) = S\left[\frac{b(\xi, \tau)}{a(\xi)}; \zeta_j, \frac{b(\zeta_j, \tau)}{a'(\zeta_j)}, j = 1, 2, \ldots, N\right]; \tag{6.3}$$

$S(\zeta, \tau)$ contains all the information necessary for reconstruction of the potentials at any time.

Following Zakharov and Shabat [19], the reconstruction of the scattering potential reduces to the solution of the linear Gel'fand-Levitan integral equation of Marchenko type

$$K_1(s, y; \tau) - F^*(s + y, \tau) - \int_s^\infty K_2^*(s, w; \tau)F^*(w + y; \tau) \, dw = 0, \tag{6.4}$$

where $K_2^*(s, w; \tau) = -\int_s^\infty K_1(s, r; \tau)F(r + w; \tau)\,dr$ and $y \geqslant s$. The kernel is

$$F(s; \tau) = \frac{1}{2\pi} \int_{-\infty}^\infty \frac{b(\xi; \tau)}{a(\xi)} \exp(i\xi s)\,d\xi - i \sum_{j=1}^N c_j(\zeta_j; \tau)\exp(i\zeta_j s), \quad (6.5)$$

and the potential $q(s; \tau)$ is related to the dependent variable $K_1(s, y)$ as

$$q(s; \tau) = -2K_1(s, s; \tau). \tag{6.6}$$

The kernel is closely analogous to the inverse Fourier transform and clearly shows the linear summation of the continuous and discrete elements. These components are separable only in scattering transform space, where advantage may be taken of linearity and the validity of superposition.

7. The discrete inverse scattering transform

Computation of the discrete inverse scattering transform requires the discrete computation of the kernel $F(z)$ from the time evolved scattering data spectrum and the numerical solution of the Gel'fand-Levitan equation. The resultant time evolved discrete scattering potential may then be demodulated and dimensionalised to obtain the wave record at any time.

The time evolution of the scattering data spectrum in transform space is

$$\frac{b(r\Delta\xi, \tau)}{a(r\Delta\xi)} = \frac{b(r\Delta\xi, 0)}{a(r\Delta\xi)} \exp\left[4i(r\Delta\xi)^2\tau\right], \tag{7.1}$$

and

$$\frac{b(\zeta_j, \tau)}{a(\zeta_j)} = \frac{b(\zeta_j, 0)}{a(\zeta_j)} \exp\left(4i\zeta_j^2\tau\right), \tag{7.2}$$

yielding both the discrete and continuous spectra in a suitable form for computation of the kernel $F(z; \tau)$. The time τ may have any positive or negative value, a zero value for τ recovering the original record.

The continuous part of the kernel has the form of an inverse Fourier integral. The inverse FFT algorithm is potentially applicable but loses computational attraction where the number of discrete points in the data series is not an integer power of two. Greater flexibility was achieved in initial computations by

trapezoidal rule integration of the continuous spectrum, the discrete representation of the kernel being

$$F(m\Delta s) = \frac{1}{2\pi} \sum_{r=-R}^{R} \frac{b(r\Delta\xi, \tau)}{a(r\Delta\xi)} \exp(ir\Delta\xi m\Delta s) - i \sum_{j=1}^{N} c_j(\zeta_j, \tau)\exp(i\zeta_j m\Delta s),$$

$$(7.3)$$

for $m = -2M, \ldots, -1, 0, 1, \ldots, 2M$.

The Gel'fand-Levitan integral equation was reformulated as a set of simultaneous linear algebraic equations in the unknowns $K_1(s, y)$ by trapezoidal rule integration, yielding a separate linear equation for each discrete value of $y \geq s$. Adopting the discrete notation $s = S\Delta s$, $S = -M, \ldots, 0, \ldots, M$; $y = Y\Delta s$, $Y = s, \ldots, M$; $w = W\Delta s$, $W = S, \ldots, M$; $r = R\Delta s$, $R = S, \ldots, M$; $K_Y = K_1(s, y; \tau) = K_1(S\Delta s, Y\Delta s; \tau)$; $F_{S+Y} = F(s + y; \tau) = F(S\Delta s + Y\Delta s; \tau)$; $K_W^* = K_2^*(s, w; \tau) = K_2^*(S\Delta s, W\Delta s; \tau)$; equation (6.4) becomes

$$K_Y - F_{S+Y}^* - \Delta s \left[\tfrac{1}{2} K_S^* F_{S+Y}^* + \sum_{j=S+1}^{M-1} K_j^* F_{j+Y}^* + \tfrac{1}{2} K_M^* F_{M+Y}^* \right] = 0, \quad (7.4)$$

where $K_W^* = -\Delta s[\tfrac{1}{2} K_S F_{S+W} + \sum_{i=S+1}^{M-1} K_i F_{i+W} + \tfrac{1}{2} K_M F_{M+W}]$. This may be expanded as

$$K_Y - F_{S+Y}^* + \frac{\Delta s^2}{2} \left[\tfrac{1}{2} F_{S+Y}^* F_{2S} + \sum_{j=s+1}^{M-1} F_{j+Y}^* F_{S+j} + \tfrac{1}{2} F_{M+Y}^* F_{S+M} \right] K_S$$

$$+ \Delta s^2 \left[\tfrac{1}{2} F_{S+Y}^* \sum_{i=S+1}^{M-1} F_{i+S} K_i + \sum_{j=S+1}^{M-1} F_{j+Y}^* \sum_{i=S+1}^{M-1} F_{i+j} K_i + \tfrac{1}{2} F_{M+Y} \sum_{i=S+1}^{M-1} F_{i+M} K_i \right]$$

$$+ \frac{\Delta s^2}{2} \left[\tfrac{1}{2} F_{S+Y}^* F_{M+S} + \sum_{j=S+1}^{M-1} F_{j+Y}^* F_{M+j} + \tfrac{1}{2} F_{M+Y}^* F_{2M} \right] K_M = 0,$$

$$(7.5)$$

which is the linear algebraic equation in the $M - S + 1$ unknowns K_i:

$$K_Y + \tfrac{1}{2} C_{S,Y} K_S + \sum_{i=S+1}^{M-1} C_{i,Y} K_i + \tfrac{1}{2} C_{M,Y} K_M = F_{S+Y}^*, \quad (7.6)$$

where $C_{i,Y} = \Delta s^2[\tfrac{1}{2} F_{S+Y}^* F_{i+S} + \sum_{j=S+1}^{M-1} F_{j+Y}^* F_{i+j} + \tfrac{1}{2} F_{M+Y}^* F_{i+M}]$; these complex coefficients being calculated at location $Y\Delta s$ as a function only of the known discrete kernel $F(m\Delta s)$.

Equation (7.6) was reduced to lower triangular form using Gauss-Jordan elimination with pivot scaling, the back substitution step being unnecessary as only the K_S value corresponding to $K_1(s, s; \tau)$ was required. All $2M + 1$ matrices

of size m by $m(m = 2M + 1, 2M, \ldots, 1)$ must be reduced to lower triangular form, the scattering potential being related to the unknowns K_S as

$$q(S\Delta s) = -2K_S, \tag{7.7}$$

for $S = -M, \ldots, -1, 0, 1, \ldots, M$. The complex wave envelope is reconstructed as $A(m\Delta x; t) = (4/2ik_0)q(m\Delta s; \tau)$ and the discrete wave record as $H(m\Delta x, t) = \text{Re}[A(m\Delta x, t)\exp(ik_0 m\Delta x)]$ for $m = -M, \ldots, -1, 0, 1, \ldots, M$; $H(0, t)$ is then given by the reverse of equation (5.1).

8. Exploratory computations

A number of exploratory analyses on artificially generated wave records were conducted to verify the algorithms and to assess the significance of the discrete finite approximations to the infinite continuous problem. Results from one of these records, a cosine wave packet, are shown in Figure 3. Figure 3a at $t = 0$ shows the initial record, for which the computed scattering potential is shown in Figure 3b at $\tau = 0$. The computed scattering data is shown in Figure 3c, the discrete spectrum identifying a single soliton at $\xi = 0$. The lobal structure of the continuous spectrum is the direct result of the discrete resolution of the wave record, the magnitude of the lobal components being dependent on the discrete resolution as seen in Figure 4 for various discrete resolution intervals Δs. There are similarities here to the sinc function, which is the discrete Fourier transform of a rectangular data window, but the details will need to be clarified.

The consequences of discrete resolution are further illustrated in terms of the sum $aa^* + bb^*$ as a function of the dimensionless discrete resolution parameter
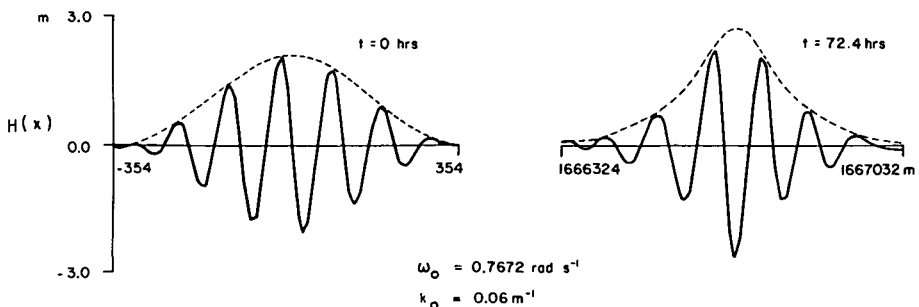

Figure 3a. Analysis, evolution and synthesis of a cosine wave packet—the wave record.

$\xi \Delta s$, as shown in Figure 5. In accordance with equation (4.4), $aa^* + bb^*$ should remain identically one for all ξ values; reasonable resolution of $aa^* + bb^*$ and hence of the scattering coefficients is possible only with $\xi \Delta s$ values less than approximately 0.3. Figure 5 has the characteristics of an efficient low pass filter. Wave components in excess of this cutoff at 0.3 are severely damped or completely filtered. This $\xi \Delta s$ dependency, which is similar in concept to the aliasing and frequency resolution phenomena encountered in the discrete Fourier transform, is a direct consequence of the discretisation; it may be accommodated in practice by appropriate selection of sampling intervals and sample lengths, in a manner similar to current practice in Fourier analysis of wave records. The low
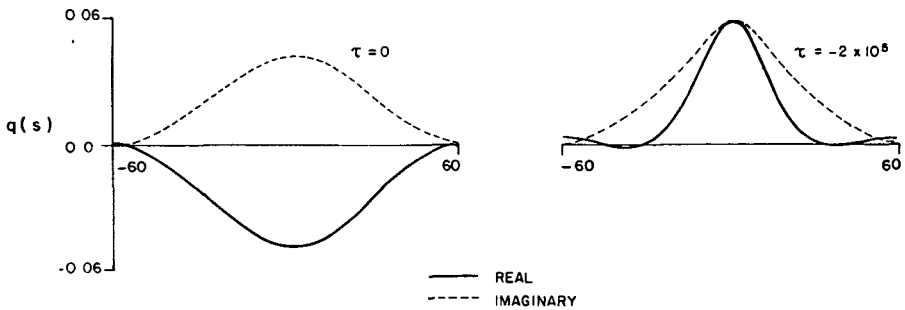

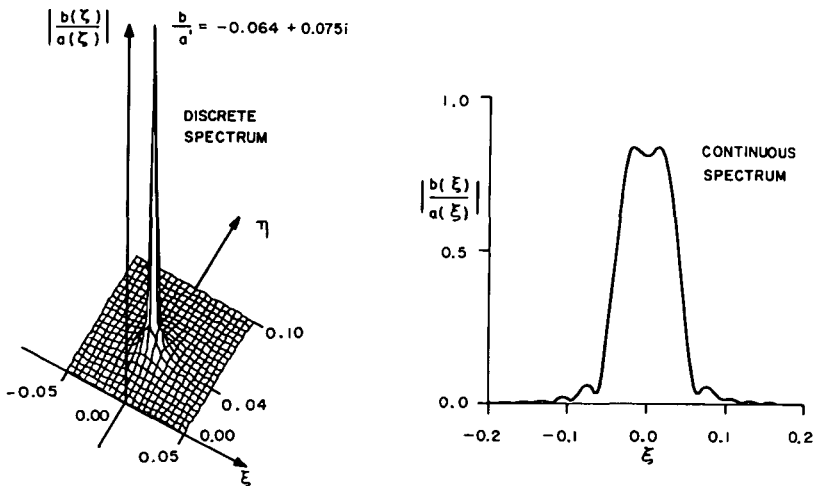Figure 3b. Analysis, evolution and synthesis of a cosine wave packet—the scattering potential.

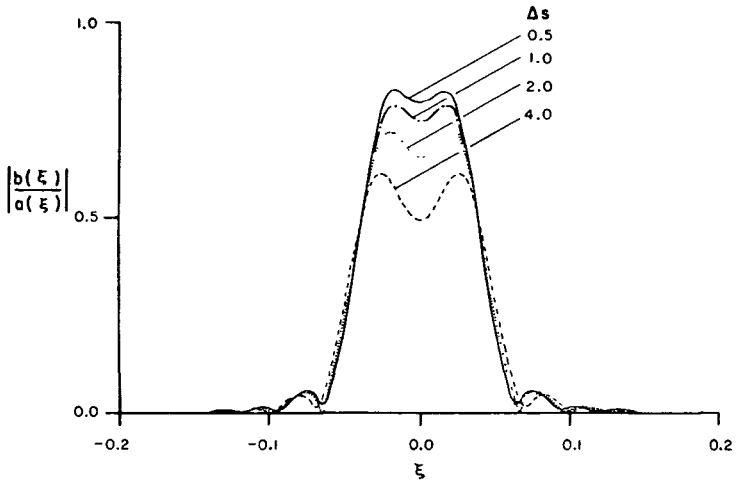Figure 3c. Analysis, evolution and synthesis of a cosine wave packet—the scattering data.

Figure 4. Influence of discrete resolution of scattering potential on the computed continuous spectrum of a cosine wave packet.
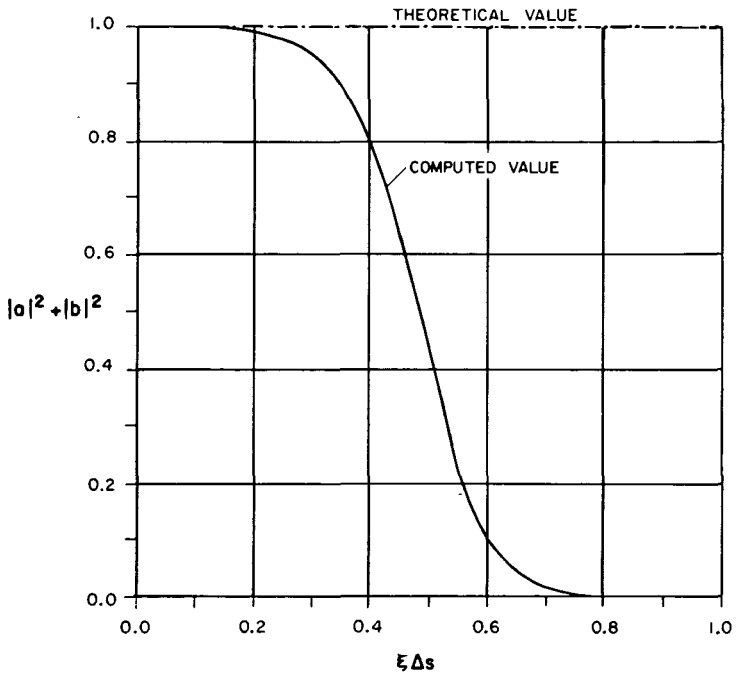

Figure 5. Numerical resolution of the discrete scattering transform.

pass filtering may not be a serious limitation as it is consistent with narrow-banded spectra, which are fundamental to the nonlinear Schrödinger equation.

The data window was also observed to influence the shape of the spectrum. Figure 6 shows the computed spectra of a sinusoidal wave record with cosine taper windows applied over various fractions J/M of the length of the record. The limiting cases of $J/M = 1.0$ and 0.2 correspond to the cosine wave packet of Figure 3a and to a sinusoidal wave record with a standard one-tenth cosine taper data window, respectively. Leakage of the continuous spectrum into the side lobes increases as the data window tends towards a rectangular window, as is also observed in Fourier analysis. As for the discrete resolution problem, the influence of the data window on the computed spectra may be accommodated and compensated in practice as it is in the computation of the Fourier transform.

Any distortion in the scattering data introduced by the discrete direct scattering transform is of course retained in the inverse transform but appropriate selection of the resolution parameters $\Delta\xi$ and $\Delta\eta$ led to successful reconstruction of the cosine wave packet at the same or a later time (Figure 3). Similar success was
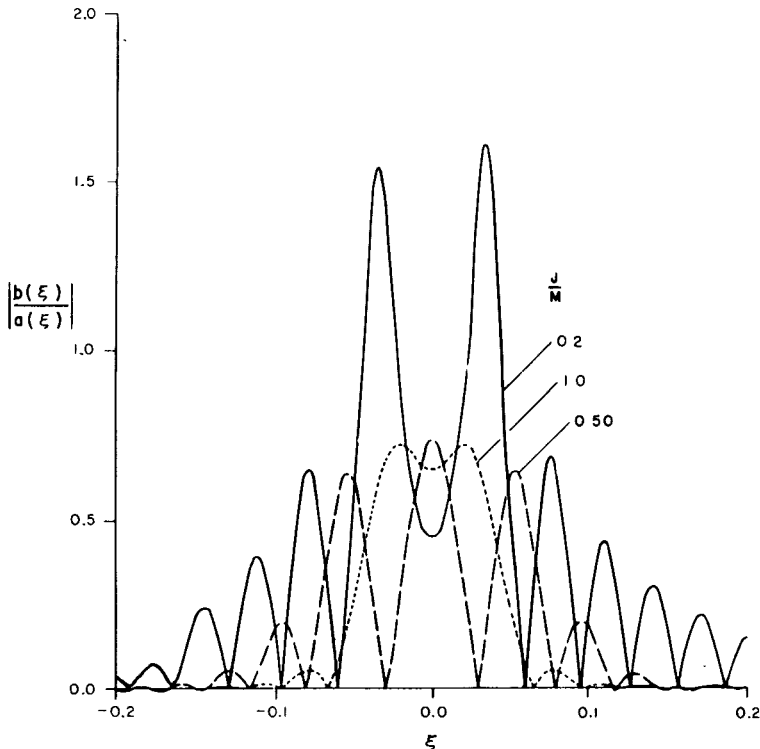

Figure 6. Influence of data window on the continuous spectrum of a cosine wave packet.

achieved with an envelope soliton record, providing adequate verification of both the discrete direct (DST) and discrete inverse (IST) scattering transform algorithms. A more detailed description of the numerical details and results has been presented by Colman and Sobey [5], together with a discussion of wave grouping and a preliminary application of the scattering transform to field records.

9. Scattering data in wave analysis

The scattering data has much to recommend it as an analysis technique for natural sea states. It has a solid foundation in the physics of finite amplitude gravity waves, being based on the nonlinear Schrödinger equation. Envelope soliton wave groups are accommodated quite naturally against a background of free wave solutions. The normal modes, the free wave and soliton components, are separable in scattering transform space and these eigenvalues are time invariant. The behaviour of the corresponding eigenfunctions for all s is not required as only the scattering data, the asymptotic ($|s| \to \infty$) behaviour of the eigenfunctions, is necessary to fully define the complex envelope $u(s, \tau)$. Furthermore the time evolution of the scattering data is independent of $u(s, \tau)$ and the corresponding nonlinear wave train is recoverable at any time, through the inverse scattering transform.

The close analogy to Fourier spectrum analysis and the Gaussian random wave model is clear and in that context the Fourier transform has become indirectly the standard summary of a natural sea state. In the context of the nonlinear Schrödinger equation it is the scattering transform, specifically the scattering data $S(\zeta, 0)$, that provides the analogous summary. The present authors have argued in [15] the potential of the scattering transform as a "third generation" wave analysis technique, that retains many of the advantages of the "second generation" Gaussian random wave model but accommodates in particular envelope soliton wave groups.

However, there remain a number of unresolved aspects associated with the possible application of the scattering data in wave analysis, the most significant of which is perhaps the limitation imposed by equation (4.5) on the validity of the scattering transform. This condition would seem to preclude uniform wave train solutions from inclusion among the scattering data. A background of free wave or radiation components are retained, however, and the link between these wave forms and the uniform wave solutions needs further clarification. A similar limitation on the Fourier transform, equation (5.7), theoretically excludes linear uniform wave trains from Fourier spectrum analysis but this difficulty is overcome, or at least bypassed, by the need to use finite data windows to accommodate a discrete and finite record and spectrum. A more positive development is the

soliton solution presented by Ma [12], which decays instead to the uniform wave train solution at infinity (*i.e.* to equation (2.5) as $|s| \to \infty$). At the large amplitude extreme this solution is the superposition of the uniform solution and a much larger envelope soliton. At the small amplitude extreme, the Ma solution describes what Lake *et al.* [10], have termed Fermi-Pasta-Ulam recurrence, recurring modulations in the amplitude of the uniform wave train. The impact of the Ma soliton on the present analysis has not been considered in detail but it would appear to enhance the potential utility of the scattering transform in wave analysis.

An additional problem is the multi-directionality of wind seas and/or the superposition of wave trains generated by separate meteorological events. The envelope soliton is known to be unstable to three-dimensional perturbations, [14], but the nature of this instability is not yet known. It may well be evolutionary rather than explosive, in a manner similar to the uniform wave train solutions, and the scattering analysis may remain relevant.

These unresolved aspects of the approach foreshadow many problems in its possible widespread application to analysis and synthesis of natural wave trains. However, it is pertinent to remember that many of these problems are similar in concept to those inherent in the now commonly used Gaussian random wave model and associated Fourier analysis. The application of the scattering data to wave analysis would need to accommodate or tolerate many of these problems in a similar way. In the long term however, the success of the scattering data in representing real sea states will be the only measure of its ultimate usefulness.

10. Conclusions

The nonlinear Schrödinger equation describes the evolution of weakly nonlinear wave trains, of which there are two distinct classes—uniform wave trains and envelope solitons. The Zakharov-Shabat scattering transform is an exact solution technique for the nonlinear Schrödinger equation and the uniform wave train and envelope soliton solutions are separable in scattering transform space. The scattering transform is a nonlinear analogue of the linear Fourier transform and the scattering data, the scattering transform of the initial data, is a potential alternative to the common Fourier transform/variance spectrum representation of a wave record.

The Zakharov-Shabat scattering transform is applicable to infinite, continuous records. Both the direct and inverse transforms are defined for finite, discrete records, as typically available from wave buoys. Proven algorithms are presented for the numerical computation of both the direct and inverse transforms. The

influence of both discrete resolution and the data window on the numerical transforms are considered; not unexpectedly, the analogy with the Fourier transform is maintained, although the details are of course different.

References

[1] M. J. Ablowitz, D. J. Kaup, A. C. Newell and H. Segur, "The inverse scattering transform — Fourier analysis for nonlinear problems", *Stud. Appl. Math.* 53 (1974), 249–315.

[2] B. A. Bolt and D. R. Brillinger, "Estimation of uncertainties in eigenspectral estimates from decaying geophysical time series", *Geophys. J. Roy. Astron. Soc.* 59 (1979), 593–603.

[3] E. O. Brigham, *The fast Fourier transform* (Prentice-Hall, Englewood Cliffs, 1974).

[4] R. V. Churchill, *Complex variables and applications* (McGraw-Hill, New York, 2nd edition, 1960).

[5] E. J. Colman and R. J. Sobey, "Analysis and synthesis of natural wave trains in deep water", *Dept. Civil and Systems Engrg., James Cook Univ. Res. Bull.* CS23 (1982).

[6] A. Davey and K. Stewartson, "On three-dimensional packets of surface waves", *Proc. Roy. Soc. London Ser. A* 338 (1974), 101–110.

[7] R. Deutsch, *Nonlinear transformations of random processes* (Prentice-Hall, Englewood Cliffs, 1962).

[8] C. S. Gardner, J. M. Greene, M. D. Kruskal and R. M. Miura, "Method for solving the Korteweg-de Vries equation", *Phys. Rev. Lett.* 19 (1967), 1095–1097.

[9] H. Hasimoto and H. Ono, "Nonlinear modulation of gravity waves", *J. Phys. Soc. Japan* 33 (1972), 805–811.

[10] B. M. Lake, H. C. Yuen, H. Rungaldier and W. E. Ferguson, "Nonlinear deep-water waves: theory and experiment, Part 2. Evolution of a continuous wave train", *J. Fluid Mech.* 83 (1977), 49–74.

[11] M. J. Lighthill, *Introduction to Fourier analysis and generalised functions* (Cambridge University Press, Cambridge, 1958).

[12] Y.-C Ma, "The perturbed plane-wave solution of the cubic Schrödinger equation", *Stud. Appl. Math.* 60 (1979), 43–58.

[13] F. J. Resch and R. Abel, "Spectral analysis using Fourier transform techniques", *Internat. J. Numer. Methods. Engrg.* 9 (1975), 869–902.

[14] P. G. Saffman and H C. Yuen, "Stability of a plane soliton to infinitesimal two-dimensional perturbation", *Phys. Fluids* 21 (1978), 1450–1451.

[15] R. J. Sobey and E. J. Colman, "Natural wave trains and scattering transform", *J. Waterway Port Coastal and Ocean Div. ASCE* 108 (1982), 272–290.

[16] H. Tennekes and J. L. Lumley, *A first course in turbulence* (MIT Press, Cambridge, Mass., 1972).

[17] H. C. Yuen and B. M. Lake, "Nonlinear deep water waves: theory and experiment", *Phys. Fluids* 18 (1975), 956–960.

[18] V. E. Zakharov, "Stability of periodic waves of finite amplitude on the surface of a deep fluid", *J. Appl. Mech. Tech. Phys.* 9 (1968), 86–94.

[19] V. E. Zakharov and A. B. Shabat, "Exact theory of two dimensional self focussing and one dimensional self modulation of waves in nonlinear media", *Soviet Phys. JETP* 34 (1972), 62–69.